

# Adaptive Trajectory Planning and Optimization at Limits of Handling

Lars Svensson<sup>1</sup>, Monimoy Bujarbaruah<sup>2</sup>, Nitin Kapania<sup>3</sup> and Martin Törngren<sup>1</sup>

**Abstract**—As deployment of automated vehicles increases, so does the rate at which they are exposed to critical traffic situations. Such situations, e.g. a late detected pedestrian in the vehicle path, require operation at the handling limits in order to maximize the capacity to avoid an accident. Also, the physical limitations of the vehicle typically vary in time due to local road and weather conditions. In this paper, we tackle the problem of trajectory planning and control at the limits of handling under time varying constraints, by adapting to local traction limitations. The proposed method is based on Real Time Iteration Sequential Quadratic Programming (RTI-SQP) augmented with state space sampling, which we call Sampling Augmented Adaptive RTI-SQP (SAA-SQP). Through extensive numerical simulations we demonstrate that our method increases the vehicle’s capacity to avoid late detected obstacles compared to the traditional planning/tracking approaches, as a direct consequence of safe operating constraint adaptation in real time.

## I. INTRODUCTION

Automated driving and advanced driver assistance systems technology is developed and deployed around the world as means of improving mobility and safety in the transportation system. Research in motion planning and control of automated road vehicles has matured rapidly in recent years and numerous academic works have presented algorithms for motion planning and control in general driving scenarios [1]–[4]. The traffic environment in which automated vehicles operate is inherently unpredictable and therefore critical situations will eventually occur regardless of the behavior of the ego vehicle. With increased deployment in real environments, the system’s capability to handle critical situations becomes increasingly important. To preserve safety of passengers and other road users in such critical situations, the automated driving functionality is required to operate the vehicle near the limits of its physical capabilities in order to perform emergency stops or evasive maneuvers optimally. Conservative assumptions about the physical capacity of the vehicle reduces the set of considered maneuvers, which may lead to reduced safety in a critical situation.

Due to computational limitations, the planning and control problem is generally divided into hierarchical levels with gradually decreasing planning horizon and increasing model fidelity. A dynamic model, including tire force modelling is typically only used for trajectory tracking [1], [2], whereas local trajectory planning typically uses less sophisticated

models, such as the kinematic bicycle model or the point mass model [3], [4]. Not being able to precisely represent the dynamic limitations in the local planner presents a potential problem when motion planning close to the dynamic limits of the vehicle in one of two ways. First, over-estimating the dynamic capabilities may lead to poor tracking performance in the controller, possibly resulting in collision. Second, under-estimating the dynamic capability may cause failure to select an available collision free maneuver. Several works have been proposed to mitigate this discrepancy by employing pre-computed motion primitives in the local planner for which the dynamic limitations are considered [5], [6]. However, the dynamic capabilities of road vehicles are typically prone to substantial local variations in terms of the tire-road friction coefficient [7], rendering pre-computed motion primitives suboptimal or infeasible in most cases. Hence, accurate estimation of dynamic capabilities, coupled with adaptive optimal motion planning and control is key in order to fully utilize the physical capabilities of the vehicle. In this work, we assume a state-of-the-art solution of the tire-road friction estimation problem [7]–[9], and focus on subsequent motion planning and control, utilizing the up-to-date friction estimation.

In this paper, we propose an integrated framework for vehicle local planning and control, in which the dynamic constraints of the vehicle can be adapted at run-time. The method utilizes a combination of state space sampling [10] and adaptive model predictive control (MPC) [11], employed in a Real Time Iteration Sequential Quadratic Programming (RTI-SQP) fashion [12]. We demonstrate in numerical simulations that the method increases the vehicle’s capacity to avoid obstacles in critical situations compared to an equivalent non-adaptive method as well as a traditional modular planning-tracking scheme. In summary, this work presents a unified trajectory planning and optimization algorithm, which we call Sampling Augmented Adaptive RTI-SQP (SAA-SQP), bearing the following contributions:

- 1) A sampling based strategy for adaptive motion planning at the limits of handling, which incorporates the knowledge of vehicle model and operating constraints. For this planner, the time-varying tire-road friction limitation is handled as a time-varying adaptive input constraint, utilizing concepts from adaptive MPC.
- 2) A real-time trajectory optimization algorithm based on RTI-SQP, for optimizing planned trajectories from 1) in environments with obstacles. The proposed algorithm avoids potential infeasibility and local minima, while utilizing full dynamic capabilities of the vehicle via the

<sup>1</sup> L.Svensson and M.Törngren are with the Mechatronics and Embedded Control Systems, KTH Royal Institute of Technology, Stockholm, Sweden. {larsvens, martint}@kth.se

<sup>2</sup>M. Bujarbaruah is with the Model Predictive Control Laboratory at University of California Berkeley, USA. monimoyb@berkeley.edu

<sup>3</sup>N. Kapania is with the Dynamic Design Laboratory at Stanford University, USA. nkapania@stanford.edu

adaptive inputs constraints from 1).

The paper is organized as follows: Section II gives a brief overview of related work. Section III introduces models, constraints and an ideal motion planning problem, which is used as a baseline for the proposed algorithm in Section IV. Finally, we demonstrate simulation results in Section V.

## II. RELATED WORK

Research in motion planning and control at the handling limits was influenced by research in the racing community. Through the use of nonlinear programming, Perantoni et al. [13] were able to compute the time-optimal speed profile and racing line for an entire race track, although computational limits required the trajectories to be computed offline. Kapania and Gerdes [14] presented an experimentally validated algorithm that reduced computational expense by breaking down the combined lateral/longitudinal vehicle control problem into two sequential subproblems that were solved iteratively.

Another optimization based approach to the autonomous racing problem is to repeatedly solve a Constrained Finite Time Optimal Control (CFTOC) problem online. Liniger et al. [6] utilizes the Real Time Iteration Sequential Quadratic Programming (RTI-SQP) paradigm [15] to jointly solve the trajectory planning and control problems. Rosolia [16] applied learning MPC to minimize lap completion time, given data from previous laps, while satisfying safety constraints. Building on the experiences from the racing application, Gray et al. [17] considered motion planning at the handling limits for obstacle avoidance, generating a high-level motion plan from a four-wheel dynamic model and a low-level plan using MPC. Zhang et al. [18] re-formulate the collision avoidance constraints in the dual variable space, which results in a smooth (but still, non-convex) optimization problem. A predictive control approach was also utilized by Funke et al. [19] and Brown et al. [20] to provide collision-free trajectories while maintaining vehicle stability. A practical drawback of purely optimization-based motion planning techniques pointed out by Ziegler et al. [3] is that they struggle in situations where the motion planning problem contains discrete decision making (e.g. to go left or right of an obstacle). In specific cases [6], [20], this can be remedied by a high level path planner based on a method such as dynamic programming. However, to the best of our knowledge, a generalized solution for this problem without loss of optimality w.r.t. the dynamic capabilities of the vehicle has yet to be presented.

Hence for practicality, state space sampling methods such as those presented by Howard et al. [10] are widely used in industry for collision avoidance. The core concept of the method is as follows. A grid is defined in the terminal state of the planning horizon and a set of two point boundary value problems are solved between the initial state and each sampled terminal state, generating a trajectory set. Dynamic constraints are not considered in the generation of the trajectory set. Instead, a dynamic feasibility check is done in conjunction with the collision check for each trajectory.

Werling et al extended the method in [21] by generating the trajectory set in a road-aligned coordinate frame, [22], and in [4] by introducing a terminal manifold to improve the selection of terminal states. It has been shown that the method is well suited for planning in scenarios including discrete decisions. However, even though it reliably produces feasible maneuvers, they are suboptimal w.r.t. the physical capabilities of the vehicle.

An intuitive way to reduce suboptimality of the trajectories in the set is to solve the two-point boundary value problem offline, using a dynamic model. This method has been demonstrated successfully in several previous works [5], [6]. However, this approach prohibits online model adaptation, since the trajectories in the pre-computed library assumes a static vehicle model.

On the other hand, to account for local variations in physical capabilities of the vehicle, we draw from developments in the field of adaptive control. Predictive control under model uncertainty has been well-studied recently [11], [23]–[26]. Such frameworks allow the system to dynamically re-plan safer and more cost efficient trajectories with time, as additional model information available from data is provided to the MPC optimization problem. We leverage this notion of *adaptive MPC* in our work as well, by utilizing updated vehicle model information to adapt the constraints to account for time-varying traction limitations. With extensive numerical examples, we highlight that this method of recursive model adaptation in MPC improves the capacity to avoid obstacles under time-varying road conditions.

## III. PROBLEM FORMULATION

In this paper, we tackle the problem of real-time trajectory planning and control of a vehicle at its limits of handling, under time varying dynamic constraints. The controller synthesis is done by solving an optimization problem in a receding horizon fashion. In the following section we introduce the model and time varying constraints of the optimization problem.

*Vehicle Model:* Throughout this paper we consider a dynamic bicycle model expressed in a road aligned coordinate frame. The state propagation is described in (1).

$$\dot{s} = \frac{v_x \cos(\Delta\psi) - v_y \sin(\Delta\psi)}{1 - d\kappa_c}, \quad (1a)$$

$$\dot{d} = v_x \sin(\Delta\psi) + v_y \cos(\Delta\psi), \quad (1b)$$

$$\Delta\dot{\psi} = \dot{\psi} - \kappa_c \frac{v_x \cos(\Delta\psi) - v_y \sin(\Delta\psi)}{1 - d\kappa_c}, \quad (1c)$$

$$\ddot{\psi} = \frac{1}{I_z} (l_f F_{yf} - l_r F_{yr}), \quad (1d)$$

$$\dot{v}_x = \frac{1}{m} F_x, \quad (1e)$$

$$\dot{v}_y = \frac{1}{m} (F_{yf} + F_{yr}) - v_x \dot{\psi}. \quad (1f)$$

$s$  denotes the curvilinear abscissa i.e., the progression of the vehicle along the centerline of the lane with curvature  $\kappa_c$  at  $s$ .  $d$  represents the normal distance from the centerline

at  $s$  to the center of mass of the vehicle.  $\Delta\psi$  denote the vehicle orientation relative to the centerline tangent at  $s$ .  $\dot{\psi}$ ,  $v_x$  and  $v_y$  denote yaw rate, longitudinal and lateral velocities respectively. The inputs of the model are  $F_{yf}$ , the lateral force on the front tire and  $F_x$ , the combined longitudinal force on the front and rear tires.  $m$ ,  $I_z$ ,  $l_f$  and  $l_r$  are physical vehicle parameters. For the purposes of this paper we assume that effects of longitudinal load transfer, bank angle and grade angle of the road are small. The derivation of the vehicle model is omitted [9]. Now, we compactly write (1) as  $\dot{x} = f_c(x, u)$  where  $x = [s \ d \ \Delta\psi \ \dot{\psi} \ v_x \ v_y]^\top$  and  $u = [F_{yf} \ F_x]^\top$ . We then discretize (1) using forward Euler discretization,  $x_{t+1} = x_t + T_s f_c(x_t, u_t)$  with sampling time  $T_s$ , to get  $x_{t+1} = f(x_t, u_t)$ .

**Ideal Optimal Control Problem:** For trajectory planning and control synthesis, we wish to solve the following Constrained Finite Time Optimal Control (CFTOC) problem at all time instances  $t$ :

$$\begin{aligned} \min_{u_{0|t}, \dots, u_{N-1|t}} \quad & p(x_{N|t}) + \sum_{k=0}^{N-1} q(x_{k|t}, u_{k|t}) \\ \text{s.t.} \quad & x_{k+1|t} = f(x_{k|t}, u_{k|t}), \\ & x_{k|t} \in \mathcal{X}_t, \quad u_{k|t} \in \mathcal{U}_t(\mu_t), \\ & x_{0|t} = x_t, \quad \forall k = 0, \dots, N-1, \end{aligned} \quad (2)$$

where  $[x_{0|t}, \dots, x_{N|t}]^\top$  at time  $t$ , denote the predicted states along a prediction horizon of length  $N$ , when the predicted input sequence  $[u_{0|t}, \dots, u_{N-1|t}]^\top$  is applied through vehicle model  $f(\cdot, \cdot)$ . The inputs  $u_{k|t}$  for all  $k \in \{0, N-1\}$  are bounded by the sets  $\mathcal{U}_t(\mu_t) \subseteq \mathbb{R}^m$  to account for local dynamic limitations of the vehicle.  $\mu_t$  is the identified tire-road friction coefficient. The sets  $\mathcal{X}_t \subseteq \mathbb{R}^n$  represent collision free states of the vehicle with respect to drivable area, static and dynamic obstacles.  $q(\cdot, \cdot)$  and  $p(\cdot)$  denote the positive definite running cost and final cost functions respectively. After solving (2) at each time  $t$ , the first optimal input  $u_t = u_{0|t}^*$  is to be applied in closed loop and then (2) is to be solved at next time  $t+1$ , as per the receding horizon strategy. Notice that the problem (2) is formulated with time varying constraints  $\mathcal{U}_t(\mu_t)$  and  $\mathcal{X}_t$ . Time variation in  $\mathcal{X}_t$  is required to represent predicted movement of dynamic obstacles. Time variation in  $\mathcal{U}_t(\mu_t)$  is introduced to account for local variations in the physical capabilities of the vehicle due to, tire-road friction variations. We hypothesize that adapting to local road conditions and acting optimally with respect to the associated physical limitations at its limits of handling, will improve the capacity of the vehicle to avoid collision with suddenly appearing obstacles.

**Adaptive Constraints:** The maximum horizontal force that can be exerted between a tire and the road at time  $t$  is determined by the normal force,  $F_z$ , and the tire-road friction coefficient  $\mu_t$ . The boundary of combined lateral and longitudinal forces on a single tire is referred to as a friction circle [9]. For our dynamic bicycle model we have that

$$F_{yf}^2 + F_{xf}^2 \leq (\mu F_{zf})^2, \quad F_{yr}^2 + F_{xr}^2 \leq (\mu F_{zr})^2. \quad (3)$$

Considering the control inputs of (1) and assuming that effects of longitudinal load transfer are small, the friction

circle constraint is satisfied if the pair of control inputs  $F_{yf}$  and  $F_x$  are inside an ellipse with half-axes  $\mu F_{zf}$  and  $\mu F_{zr}$ . For computational tractability of (2), we represent the input constraints as a set of affine constraints. For that reason, we determine a polytope  $\mathcal{U}_1(\mu)$  that under-approximates the ellipse. Lower and upper bounds in  $F_{yf}$  and  $F_x$  due to limits in steering angle and motor torque are represented as a second polytope  $\mathcal{U}_2$ . The final input constraint polytope is computed as the intersection  $\mathcal{U}(\mu) = \mathcal{U}_1(\mu) \cap \mathcal{U}_2 = \{u : H^\mu u \leq h^\mu\}$ , illustrated in Fig. 1. In the next section, we use

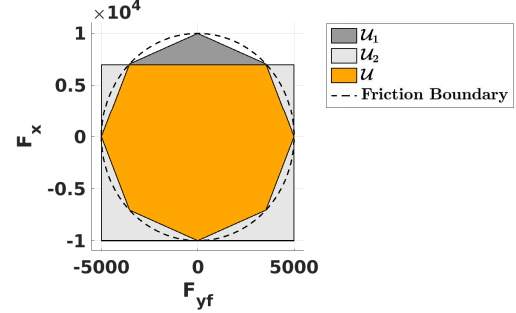


Fig. 1: Adaptive input constraint polytope capturing local limitations of tire forces. The size of  $\mathcal{U}(\mu)$  varies with the identified parameter  $\mu$

these parametric ( $\mu$  dependent) adapted input constraints to formulate a trajectory planning and optimization algorithm, which attempts to solve (2) in real-time.

#### IV. SAMPLING AUGMENTED ADAPTIVE RTI-SQP

There are majorly two practical problems with the ideal optimal control synthesis formulation in (2), namely:

- (i) A direct solution to (2) using a nonlinear solver would be prone to getting stuck in local minima, when the problem contains discrete decision making (e.g., to go left or right of an obstacle [3]). This can render the approach computationally intractable.
- (ii) Even if (2) is tractably reformulated, due to adaptive nature of the constraints, potential issues of feasibility of reformulation of (2) might arise [27], as a result of discrepancy between  $\mathcal{U}_t(\mu_t)$ ,  $\mathcal{X}_t$  and dynamics  $f(x_t, u_t)$ .

To address these problems, we propose the Sampling Augmented Adaptive RTI-SQP (SAA-SQP) algorithm, which decomposes the method of solving (2) into two distinct steps: *feasible trajectory planning* and *trajectory optimization*. The approach augments the existing RTI-SQP [15] strategy with state space sampling [10].

For the *feasible trajectory planning* step, we modify the state space sampling method in [10] to handle adaptive nature of actuation constraints (defined in Section III, Fig. 1), while satisfying vehicle dynamics (1). This incorporation of real time constraint adaptation at vehicle limits of handling, repeatedly generates a large set of feasible sampled trajectories at each time step. Unlike conventional RTI-SQP, the presence of this set of planned trajectories provides a systematic method for warmstarting the subsequent *trajectory optimization*, remedying problem (i) defined above.

In the *trajectory optimization* step, we define state constraints  $\mathcal{X}_t$  w.r.t. deviations from feasible planned trajectories. As these both trajectory planner and optimizer use the same vehicle model  $f(x_t, u_t)$  and adapted constraints  $U_t(\mu_t)$ , one planned trajectory is *guaranteed* to be a feasible solution for the *trajectory optimization* problem. Hence, (i) is resolved. In the following two sub-sections we elaborate the details of these two aforementioned steps of the algorithm.

### A. State Space Sampling & Trajectory Selection

To obtain a feasible and near-optimal solution to (2), we first utilize state space sampling [10]. The purpose of this step is to provide adequate warmstarting options for the subsequent trajectory optimization problem, while being cognizant of time variations in operating constraints. We first compute the initial state of the vehicle in the road aligned frame  $[s, d, \Delta\psi, \dot{\psi}, v_x, v_y] \mapsto [s_0, d_0, \dot{s}_0, \dot{d}_0, \ddot{s}_0, \ddot{d}_0]$ . We define a set of terminal states  $[s_T, d_T, \dot{s}_T, \dot{d}_T, \ddot{s}_T, \ddot{d}_T]$  from a grid of terminal times  $T$  and terminal lateral deviations from the lane centerline  $d_T$ . Then, for each terminal state, a trajectory from the initial state to the terminal state is determined by a piecewise linear function in  $s_t$  and a quintic polynomial in  $d_t$ . The coefficients of such a quintic polynomial  $d_t = a_0 + a_1t + a_2t^2 + a_3t^3 + a_4t^4 + a_5t^5$  can be efficiently computed by solving

$$\begin{bmatrix} 1 & 0 & 0 & 0 & 0 & 0 \\ 0 & 1 & 0 & 0 & 0 & 0 \\ 0 & 0 & 1 & 0 & 0 & 0 \\ 1 & T & T^2 & T^3 & T^4 & T^5 \\ 0 & 1 & 2T & 3T^2 & 4T^3 & 5T^4 \\ 0 & 0 & 2 & 6T & 12T^2 & 20T^3 \end{bmatrix} \begin{bmatrix} a_0 \\ a_1 \\ a_2 \\ a_3 \\ a_4 \\ a_5 \end{bmatrix} = \begin{bmatrix} d_0 \\ \dot{d}_0 \\ \ddot{d}_0 \\ d_T \\ \dot{d}_T \\ \ddot{d}_T \end{bmatrix}.$$

Each trajectory is discretized in time and transformed to a state trajectory of the vehicle, satisfying dynamics (1) smoothly. This transformation  $\hat{\gamma} = [s, d, \dot{s}, \dot{d}, \ddot{s}, \ddot{d}] \mapsto \hat{x} = [s, d, \Delta\psi, \dot{\psi}, v_x, v_y]$  is computed in closed form. Calculations are available in [4].

Following the above transformation  $\hat{\gamma} \mapsto \hat{x}$ , we loop through the planned trajectory set at any time  $t$  over a finite prediction horizon of length  $N$ , checking feasibility of dynamic constraints (see Fig. 1) and avoidance of collisions. The adaptive force constraints are checked by computing the equivalent tire forces of each trajectory and checking them with respect to constraints  $U_t(\mu_t)$ . For trajectories passing this check, we evaluate a cost metric

$$J(\hat{X}_t) = \hat{x}_{N|t}^\top Q_f \hat{x}_{N|t} + \sum_{k=0}^{N-1} \hat{x}_{k|t}^\top Q \hat{x}_{k|t} + \hat{u}_{k|t}^\top R \hat{u}_{k|t}, \quad (4)$$

where  $\hat{X}_t = \{(\hat{x}_{k|t}, \hat{u}_{k|t}), k \in \{0, N\}\}$  denotes a planned trajectory (suboptimal) rolled out by the state-space sampling planner, which satisfies the vehicle dynamics  $\hat{x}_{k+1|t} = f(\hat{x}_{k|t}, \hat{u}_{k|t})$ ,  $k \in \{0, N\}$ . The matrices  $Q, Q_f, R > 0$  are selected such that the cost reflects the overall objective. The lowest cost sampled trajectory at  $t = 0$  i.e.  $\hat{X}_0^* = \{(\hat{x}_{k|0}^*, \hat{u}_{k|0}^*), k \in \{0, N\}\}$  (where  $\hat{X}_0^* = \arg \min_X J(\hat{X}_0) = (\hat{x}_{k|0}^*, \hat{u}_{k|0}^*), k \in \{0, N\}$ ) is selected for the subsequent

trajectory optimization at time  $t = 0$  to obtain the optimal  $X_0^* = \{(x_{k|0}^*, u_{k|0}^*), k \in \{0, N\}\}$ . From  $t = 1$  onward,  $\hat{X}_t^* = \arg \min_X (J(\hat{X}_t), J(X_{t-1}^*))$ . That is, the forward shifted optimal trajectory  $X_{t-1}^* = \{(x_{k|t-1}^*, u_{k|t-1}^*), k \in \{1, N\}\}$  from the previous iteration of the trajectory optimization is included in the selection on equal terms with the sampled trajectories  $\hat{X}_t$  for current time step.

*Remark 1:* In case  $X_{t-1}^*$  is selected as  $\hat{X}_t^*$ , the algorithm behaves as standard RTI-SQP [15].

Although dynamically feasible and optimal within the sampled set,  $\hat{X}_t^*$  will be suboptimal due to the structure imposed by the polynomials defining the trajectory. We will later illustrate this in Section V. Hence, we employ trajectory optimization using RTI-SQP to obtain an optimal trajectory  $X_t^*$  from the initialized suboptimal trajectory  $\hat{X}_t^*$  for all  $t \geq 0$ , rather than simply tracking suboptimal  $\hat{X}_t^*$ .

### B. Trajectory Optimization

As stated in problem (i) in the beginning of this section, the ideal adaptive CFTOC problem (2) is non-convex, so prone to getting stuck in local minima. However, solving (2) locally around the feasible but suboptimal trajectory  $\hat{X}_t^*$  can be done efficiently using a convex Quadratic Program (QP) approximation. We obtain the QP approximation of (2) through the linear time varying model predictive control paradigm [15]. At any given time  $t$ , the model and constraints in (2) are linearized around  $\hat{X}_t^*$ . Then, for one iteration of the algorithm, the following reformulated optimization problem is solved once at each time step  $t$ , instead of solving (2):

$$\begin{aligned} \min_{u_{0|t}, \dots, u_{N-1|t}} \quad & J(x_{k|t}, u_{k|t}) + \sigma_t^\top \beta \sigma_t \\ \text{s.t.} \quad & x_{k+1|t} = A_{k|t}(\Delta x_{k|t}) + B_{k|t}(\Delta u_{k|t}) + \hat{x}_{k+1|t}^*, \\ & H_t^\mu u_{k|t} \leq h_t^\mu, \\ & s_t^{\min} - \sigma_s \leq s_{k|t} \leq s_t^{\max} + \sigma_s, \\ & d_t^{\min} - \sigma_d \leq d_{k|t} \leq d_t^{\max} + \sigma_d, \\ & v_x^{\min} - \sigma_{v_x} \leq (v_x)_{k|t} \leq v_x^{\max} + \sigma_{v_x}, \\ & \forall k = 0, \dots, N-1, \\ & x_{0|t} = x_t, \\ & \sigma_t^s \leq 0, \sigma_t^d \leq 0, \sigma_t^{v_x} \leq 0, \end{aligned} \quad (5)$$

where  $[x_{1|t}, \dots, x_{N|t}]$  are predicted states obtained in open loop at time  $t$ , after applying the predicted input sequence  $[u_{0|t}, \dots, u_{N-1|t}]$  to the linearized system, and  $[\Delta x_{k|t}, \Delta u_{k|t}] = [x_{k|t} - \hat{x}_{k|t}^*, u_{k|t} - \hat{u}_{k|t}^*]$  for all  $k \in \{0, N-1\}$ . The linearized system model matrices are given as  $A_{k|t} = \frac{\delta f}{\delta x} \Big|_{(\hat{x}_{k|t}^*, \hat{u}_{k|t}^*)}$ ,  $B_{k|t} = \frac{\delta f}{\delta u} \Big|_{(\hat{x}_{k|t}^*, \hat{u}_{k|t}^*)}$ .

State constraints  $\hat{X}_t^* = \{s_t^{\min} - \sigma_t^s \leq s_{k|t} \leq s_t^{\max} + \sigma_t^s, d_t^{\min} - \sigma_t^d \leq d_{k|t} \leq d_t^{\max} + \sigma_t^d, v_x^{\min} - \sigma_t^{v_x} \leq (v_x)_{k|t} \leq v_x^{\max} + \sigma_t^{v_x}\}$  in (5) are selected, such that the deviation from  $\hat{X}_t^*$  is bounded. The constraints are softened with slack variables  $\sigma_t$  to maintain feasibility of (5) and any constraint violation is heavily penalized by  $\beta \gg 0$ . In the vicinity of obstacles and lane boundaries, the bounds on  $s$  and  $d$  are

adjusted accordingly. Hence, the number of constraints is independent of the number of obstacles.

The same cost function  $J(\cdot)$  as in the trajectory selection (shown in (4)) is employed, with the addition of the term  $\sigma^\top \beta \sigma$ , to account for slack variables in the soft state constraints. After solving (5), we apply the first input  $u_t = u_{0|t}^*$  in closed loop and resolve (5) at the next time step in a receding horizon fashion. We highlight that the novelty in (5) is two fold:

- 1) Inclusion of the adaptive constraint polytope  $\mathcal{U}(\mu_t) = \{u : H_t^\mu u \leq h_t^\mu\}$ .  $\mathcal{U}(\mu_t)$  is recomputed at every time  $t$  from the identified parameter  $\mu_t$  as per the method described in Section III, Fig. 1. This enables the resulting planned trajectory  $X_t^*$  to fully utilize the available tire force, given the current driving conditions. This improves the vehicle's capacity to avoid obstacles.
- 2) Inclusion of sampled trajectories  $\hat{X}_t$  to warmstart the optimization problem (5) at each time  $t$ . This alleviates the issue of local minima and potential infeasibility of (5). Since the same vehicle model (1) and adaptive constraints (given by  $\mathcal{U}_t(\mu_t)$ ) are applied in both trajectory selection (Section IV-A) and the trajectory optimization (Section IV-B) steps, one feasible solution to (5) is guaranteed to exist at any time  $t$ , namely  $\hat{X}_t^*$ .

We summarize the proposed Sampling Augmented Adaptive RTI-SQP (SAA-SQP) algorithm in Algorithm 1. For notations, let  $M$  represent the map features, e.g., lane boundaries and static obstacles, and  $O$  denote dynamic obstacles. We assume an existing tire-road friction estimation e.g. [7], [8] giving an estimated  $\mu_t$ .  $\mathcal{T}_t$  (defined as  $\cup_{i=1}^{\infty} \hat{X}_t^i$ ) denotes the set of sampled trajectories at time  $t$  obtained from the sampling based planner in Section IV-A.

---

**Algorithm 1** The SAA-SQP Algorithm

---

**Input:**  $x_t, X_{t-1}^*, M, O$

**Output:**  $X_t^*$

- 1:  $\mu_t \leftarrow \text{identifyFrictionCoefficient}(x_t)$
  - 2:  $\mathcal{U}_t(\mu_t) \leftarrow \text{computeAdaptiveConstraints}(\mu_t)$
  - 3:  $\mathcal{T}_t \leftarrow \text{transformToStateTrajectories}(x_t, M)$
  - 4: **for** each trajectory  $\hat{X}_t^i$  in  $[\mathcal{T}_t, X_{t-1}^*]$  **do**
  - 5:   **if**  $(\text{chkConstr}(\hat{X}_t^i, \mathcal{U}_t(\mu_t)) \wedge \text{chkColl}(\hat{X}_t^i, O))$  **then**
  - 6:      $J(\hat{X}_t^i) \leftarrow \text{evaluateCost}(\hat{X}_t^i)$
  - 7:   **end if**
  - 8: **end for**
  - 9:  $\hat{X}_t^* \leftarrow \text{selectLowestCost}(\arg J(\hat{X}_t^*))$
  - 10:  $A_{k|t}, B_{k|t} \leftarrow \text{linearizeDynamicModel}(\hat{X}_t^*)$
  - 11:  $\hat{\mathcal{X}}_{k|t} \leftarrow \text{computeStateConstraints}(\hat{X}_t^*, O, M)$
  - 12:  $X_t^* = (x_{k|t}^*, u_{k|t}^*) \leftarrow \text{opti}(\hat{X}_t^*, \mathcal{U}_t(\mu_t), \hat{\mathcal{X}}_{k|t}, A_{k|t}, B_{k|t})$
  - 13: **return**  $X_t^*$
- 

## V. RESULTS AND DISCUSSION

In this section, we demonstrate two aspects of Algorithm 1:

- (a) First, we compare adaptive and non-adaptive (depending on real time adaptation of constraints  $\mathcal{U}_t(\mu_t)$  defined

Parameter	Value
$m$	1500 kg
$I_z$	2250 kgm <sup>2</sup>
$l_f$	1.04 m
$l_r$	1.42 m
$C_{\alpha_f}$	160 kN/rad
$C_{\alpha_r}$	180 kN/rad

TABLE I: Static parameters of dynamic vehicle model used in simulations

in Section III) trajectory optimization by evaluating the realized closed loop cost  $J_{cl}(x_0) = \sum_{t=0}^{\infty} \{J(x_t, u_{0|t}^*) + \sigma_t^{*\top} \beta \sigma_t^*\}$  and empirical collision probability  $P_{\text{collision}}$  obtained from Monte Carlo simulation.

- (b) Second, we highlight the advantage of SAA-SQP for adaptive trajectory planning and optimization compared to state-of-the-art methods in terms of optimality and capacity to avoid local minima.

Simulations are conducted in closed loop with a nonlinear bicycle model with model parameters stated in Table I. The resulting quadratic programs are solved using the Yalmip interface [28] in MATLAB with the Gurobi [29] solver package.

### A. Adaptive vs. Non-Adaptive Trajectory Optimization

Given the unavoidable local variations in the actual tire-road friction  $\mu_{\text{actual}}$ , a non-adaptive motion planning strategy will use (explicitly or implicitly) an assumed friction coefficient  $\mu_{\text{assumed}}$ , that at times differs significantly from  $\mu_{\text{actual}}$ . In the selected evaluation scenario, the vehicle is driving on a curved section of road at a velocity of 15 m/s. An obstacle, which we assume is stationary, appears suddenly 15 meters ahead of the vehicle. Once the critical situation is detected, the goal of the vehicle is to reduce its speed to zero as soon as possible and come to a halt, while avoiding collision with high probability. The road conditions are divided in two cases: wet road, with  $\mu_{\text{actual}} = 0.6$  and dry road, with  $\mu_{\text{actual}} = 0.9$ . The non-adaptive trajectory optimization assumes a static friction estimate  $\mu_{\text{assumed}} = 0.75$  throughout, while our proposed SAA-SQP re-estimates this value and accordingly adapts input constraints  $\mathcal{U}_t(\mu_t)$  (see Fig. 1) in (5).

*Adapting to Lower Traction:* First we compare non-adaptive, Fig. 2a, vs. adaptive, Fig. 2b, trajectory optimization in the case where the actual traction is *below* the default assumption,  $\mu_{\text{actual}} < \mu_{\text{assumed}}$ . The realized closed loop cost  $J_{cl}$  starting from the same initial state is comparable in the two cases (3% difference), but in the non-adaptive case, the vehicle develops notably more side slip during the maneuver. The underlying cause for this is that the vehicle is unable to realize the planned motions due to saturated tire forces, as constraints are not adapted to match actual road conditions. Fig. 2a (right) shows the discrepancy between commanded tire forces (blue crosses) and real tire forces (magenta circles) and the resulting sliding motion of the vehicle (left). Whereas in Fig. 2b, we see a notably lower discrepancy

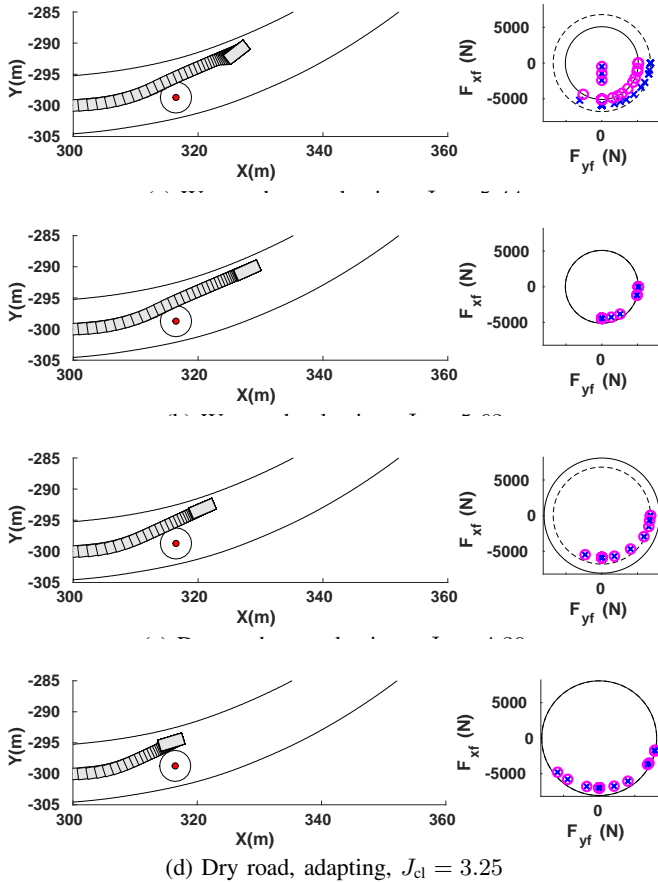


Fig. 2: Closed loop trajectories for comparison between adaptive and non-adaptive trajectory planning and control. The vehicle is depicted in gray, the suddenly appearing obstacle in red. In the force plot to the right, blue crosses denote the commanded tire forces and magenta circles denote actual tire forces. The solid and dashed black lines represent the actual and assumed friction circles respectively. Blue crosses denote the tire force command from the controller, and magenta circles denote the actual tire force realized by the vehicle.

due to real time re-estimation of  $\mu_{\text{assumed}}$  and subsequent constraint adaptation in SAA-SQP. The associated trajectory indicates that in this case, adapting gives reduced side-slip and enhanced stability during the evasive maneuver.

*Adapting to Higher Traction:* Here we compare non-adaptive Fig. 2c, vs. adaptive, Fig. 2d, trajectory optimization in the case where the actual traction is *above* the default assumption  $\mu_{\text{actual}} > \mu_{\text{assumed}}$ . We note that in this case, adapting decreases the stopping distance and the velocity at which the obstacle is passed, which is reflected by a 34% decrease in  $J_{\text{cl}}$ . The cause for this is evident from the front tire force plot in the right part of Fig. 2c. It reveals that the commanded tire forces (blue crosses) are saturated by the friction circle associated with  $\mu_{\text{assumed}}$  (dashed black), and therefore the vehicle is unable to fully utilize the available tire force without adaptation. Whereas in Fig. 2d, we see that constraint adaptation remedies the undesired saturation of commanded tire forces, resulting in a quicker, safer maneuver.

TABLE II: Results from Monte Carlo simulation of the critical obstacle avoidance scenario 100 times with an obstacle instantiated at a random position in front of the vehicle.  $\bar{J}_{\text{cl}}$  denotes the average closed loop cost and  $P_{\text{collision}}$  the collision probability over all runs. For the non-adaptive case,  $\mu_{\text{assumed}} = 0.75$  always.

Road Conditions	Strategy	$\bar{J}_{\text{cl}}$	$P_{\text{collision}}$
wet road: $\mu_{\text{actual}} = 0.6$	non-adaptive	4.79	16%
	adaptive	5.02	17%
dry road: $\mu_{\text{actual}} = 0.9$	non-adaptive	3.98	8%
	adaptive	3.29	4%

*Monte Carlo Analysis:* We generalize the trend of above results using 100 Monte Carlo simulations, and present them in Table II. The obstacle is instantiated at a random position in front of the vehicle. We evaluate the average closed loop cost  $\bar{J}_{\text{cl}}$  and the empirical collision probability over all runs  $P_{\text{collision}}$  for both wet road ( $\mu_{\text{assumed}} > \mu_{\text{actual}}$ ) and dry road ( $\mu_{\text{assumed}} < \mu_{\text{actual}}$ ) conditions. The capacity of the vehicle to avoid obstacles is improved by adapting, as is evident from the entries of  $\bar{J}_{\text{cl}}$  and  $P_{\text{collision}}$  shown in Table II.

### B. Optimality and Feasibility of SAA-SQP

In order to demonstrate enhanced optimality of realized trajectories, we compare SAA-SQP with a standard modular approach (SSS-MPC) with separated trajectory planning and tracking [2], which uses state space sampling of Section IV-A for planning and MPC for tracking the planned trajectory (which is  $\arg \min_{\mathbf{X}} J(\hat{X}_t)$ ). The key difference in the two approaches is that instead of tracking a suboptimal  $\arg \min_{\mathbf{X}} J(\hat{X}_t)$  from the planner, the SAA-SQP optimizes the selected trajectory (see Section IV-A and Algorithm 1) to obtain an optimal trajectory ( $X_t^*$ , see Section IV-B and Algorithm 1). As a result, in Fig. 3 we see that SAA-SQP stops in a shorter distance and passes the obstacle at a lower speed, which is reflected by a decrease in average closed loop cost  $\bar{J}_{\text{cl}}$ , by 42.2 % over 100 runs with a randomly instantiated obstacle.

Moreover, a direct solution of (2) using RTI-SQP is sensitive to local minima. This phenomenon is highlighted in Fig. 4. The fully converged SQP solution initialized to the left of the obstacle has a significantly higher cost 7.94, than that of the solution initialized to the right of the obstacle, which is 3.05. Thus, the solution to the left of the obstacle constitutes a local minima of (2). We observe also from Fig. 4 that SAA-SQP makes the discrete decision to go right of the obstacle and has a closed loop cost 3.156 close to the global optimum, avoiding local minima.

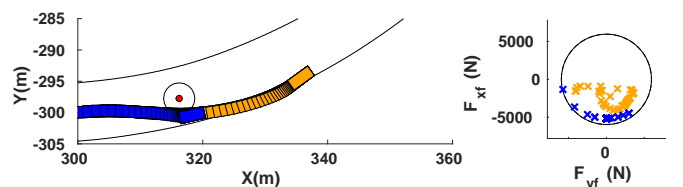


Fig. 3: Comparison of closed loop trajectories between SAA-SQP (blue) and SSS-MPC (orange)



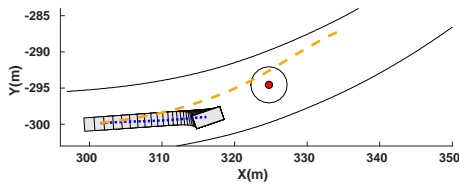


Fig. 4: Example of how SAA-SQP avoids local minima. Orange: converged SQP solution initialized left of obstacle. Blue: converged SQP solution initialized right of obstacle. Gray: Closed loop trajectory of the vehicle controlled by SAA-SQP

## VI. CONCLUSIONS AND FUTURE WORK

In order to make full use of the physical capacity of an automated vehicle to avoid collisions in critical scenarios, we propose an integrated framework for trajectory planning and optimization that adapts to current traction limitations. By updating information on operating conditions, in both planning and optimization, we ensure safe constraint adaptation and feasible trajectory generation at the limits of handling. We demonstrate that adaptation maximizes the capacity to avoid obstacles while maintaining control authority over the vehicle. Furthermore, by integrating both RTI-SQP and state space sampling, the proposed SAA-SQP algorithm represents an improvement in terms of feasibility and optimality. While not shown in this paper, the proposed method can also accommodate predicted trajectories of dynamic obstacles. [3], [4]. The focus of future work in the near-term will be addition of online tire-road friction estimation to the framework, and full-size vehicle experiments.

## ACKNOWLEDGMENT

The authors gratefully acknowledge the AutoDrive project, H2020-ECSEL and Hyundai Center of Excellence at UC Berkeley, for financial support.

## REFERENCES

- [1] B. Paden, M. Čáp, S. Z. Yong, D. Yershov, and E. Frazzoli, "A survey of motion planning and control techniques for self-driving urban vehicles," *IEEE Transactions on intelligent vehicles*, vol. 1, no. 1, pp. 33–55, 2016.
- [2] D. González, J. Pérez, V. Milanés, and F. Nashashibi, "A review of motion planning techniques for automated vehicles," *IEEE Trans. Intelligent Transportation Systems*, vol. 17, pp. 1135–1145, 2016.
- [3] J. Ziegler, P. Bender, T. Dang, and C. Stiller, "Trajectory planning for bertha—a local, continuous method," in *Intelligent Vehicles Symposium Proceedings, 2014 IEEE*. IEEE, 2014, pp. 450–457.
- [4] M. Werling, S. Kammel, J. Ziegler, and L. Gröll, "Optimal trajectories for time-critical street scenarios using discretized terminal manifolds," *The International Journal of Robotics Research*, vol. 31, no. 3, pp. 346–359, 2012.
- [5] L. Svensson, L. Masson, N. Mohan, E. Ward, A. P. Brenden, L. Feng, and M. Törnqvist, "Safe stop trajectory planning for highly automated vehicles: An optimal control problem formulation," in *2018 IEEE Intelligent Vehicles Symposium (IV)*, June 2018, pp. 517–522.
- [6] A. Liniger, A. Domahidi, and M. Morari, "Optimization-based autonomous racing of 1: 43 scale rc cars," *Optimal Control Applications and Methods*, vol. 36, no. 5, pp. 628–647, 2015.
- [7] R. Rajamani, G. Phanomchoeng, D. Piyabongkarn, and J. Y. Lew, "Algorithms for real-time estimation of individual wheel tire-road friction coefficients," *IEEE/ASME Transactions on Mechatronics*, vol. 17, no. 6, pp. 1183–1195, 2012.
- [8] F. Gustafsson, "Slip-based tire-road friction estimation," *Automatica*, vol. 33, no. 6, pp. 1087–1099, 1997.
- [9] R. Rajamani, *Vehicle dynamics and control*. Springer Science & Business Media, 2011.
- [10] T. M. Howard, C. J. Green, A. Kelly, and D. Ferguson, "State space sampling of feasible motions for high-performance mobile robot navigation in complex environments," *Journal of Field Robotics*, vol. 25, no. 6-7, pp. 325–345, 2008.
- [11] M. Bujarbaruah, X. Zhang, H. Tseng, and F. Borrelli, "Adaptive MPC for Autonomous Lane Keeping," in *14th International Symposium on Advanced Vehicle Control (AVEC)*, July 2018.
- [12] M. Diehl, H. G. Bock, and J. P. Schlöder, "A real-time iteration scheme for nonlinear optimization in optimal feedback control," *SIAM Journal on control and optimization*, vol. 43, no. 5, pp. 1714–1736, 2005.
- [13] G. Perantoni and D. J. Limebeer, "Optimal control for a formula one car with variable parameters," *Vehicle System Dynamics*, vol. 52, no. 5, pp. 653–678, 2014.
- [14] N. R. Kapania, J. Subosits, and J. C. Gerdes, "A sequential two-step algorithm for fast generation of vehicle racing trajectories," *Journal of Dynamic Systems, Measurement, and Control*, vol. 138, no. 9, p. 091005, 2016.
- [15] S. Gros, M. Zanon, R. Quirynen, A. Bemporad, and M. Diehl, "From linear to nonlinear mpc: bridging the gap via the real-time iteration," *International Journal of Control*, pp. 1–19, 2016.
- [16] U. Rosolia, A. Carvalho, and F. Borrelli, "Autonomous racing using learning model predictive control," in *2017 American Control Conference (ACC)*, May 2017, pp. 5115–5120.
- [17] A. Gray, Y. Gao, T. Lin, J. K. Hedrick, H. E. Tseng, and F. Borrelli, "Predictive control for agile semi-autonomous ground vehicles using motion primitives," in *IEEE American Control Conference (ACC)*, 2012, pp. 4239–4244.
- [18] X. Zhang, A. Liniger, A. Sakai, and F. Borrelli, "Autonomous parking using optimization-based collision avoidance," in *2018 IEEE Conference on Decision and Control (CDC)*. IEEE, 2018, pp. 4327–4332.
- [19] J. Funke, M. Brown, S. M. Erlien, and J. C. Gerdes, "Collision avoidance and stabilization for autonomous vehicles in emergency scenarios," *IEEE Transactions on Control Systems Technology*, vol. 25, no. 4, pp. 1204–1216, 2017.
- [20] M. Brown, J. Funke, S. Erlien, and J. C. Gerdes, "Safe driving envelopes for path tracking in autonomous vehicles," *Control Engineering Practice*, vol. 61, pp. 307–316, 2017.
- [21] M. Werling, J. Ziegler, S. Kammel, and S. Thrun, "Optimal trajectory generation for dynamic street scenarios in a frenet frame," in *Robotics and Automation (ICRA), 2010 IEEE International Conference on*. IEEE, 2010, pp. 987–993.
- [22] A. Micaelli and C. Samson, "Trajectory tracking for unicycle-type and two-steering-wheels mobile robots," Ph.D. dissertation, INRIA, 1993.
- [23] M. Tanaskovic, L. Fagiano, R. Smith, and M. Morari, "Adaptive receding horizon control for constrained mimo systems," *Automatica*, vol. 50, no. 12, pp. 3019–3029, 2014.
- [24] C. J. Ostafew, A. P. Schoellig, and T. D. Barfoot, "Learning-based nonlinear model predictive control to improve vision-based mobile robot path-tracking in challenging outdoor environments," in *2014 IEEE International Conference on Robotics and Automation (ICRA)*, May 2014, pp. 4029–4036.
- [25] L. Hewing and M. N. Zeilinger, "Cautious model predictive control using gaussian process regression," *arXiv:1705.10702*, 2017.
- [26] M. Bujarbaruah, X. Zhang, U. Rosolia, and F. Borrelli, "Adaptive MPC for Iterative Tasks," *57th IEEE Conference on Decision and Control (CDC)*, Dec. 2018.
- [27] T. Manrique, M. Fiacchini, T. Chambrion, and G. Millérioux, "Mpc tracking under time-varying polytopic constraints for real-time applications," in *Control Conference (ECC), 2014 European*. IEEE, 2014, pp. 1480–1485.
- [28] J. Löfberg, "Yalmip : A toolbox for modeling and optimization in matlab," in *In Proceedings of the CACSD Conference*, Taipei, Taiwan, 2004.
- [29] G. Optimization, "Inc., "gurobi optimizer reference manual," 2015," URL: <http://www.gurobi.com>, 2014.